Measurement of Line Tension on Droplets in the Submicrometer Range

ARTICLE *in* LANGMUIR · OCTOBER 2013

Impact Factor: 4.46 · DOI: 10.1021/la402932y · Source: PubMed

Langmuir

Article

pubs.acs.org/Langmuir

Measurement of Line Tension on Droplets in the Submicrometer Range

Lars-Oliver Heim* and Elmar Bonaccurso

Center of Smart Interfaces, Technical University Darmstadt, Petersenstr. 17, 64287 Darmstadt, Germany

Supporting Information

ABSTRACT: Wetting is a universal phenomenon in nature and of interest in fundamental research as well as in engineering sciences. Usually, wetting of solid substrates by liquid drops is described by Young's equation, which relates the contact angle between the liquid and the substrate to the three interfacial tensions. This concept has been widely used and confirmed for macroscopic droplets. On the contrary, it is still matter of debate to what extent this concept is able to explain relations on the micrometer scale and below. The so-called extended Young's equation, which takes account of the specific arrangement of the molecules in the three-phase contact line by implementing a term called "line tension", is frequently used to characterize deviations from the "ideal" Young's case. In this work we tried to look into the dependence of measured contact angles of droplets on their size for a close to ideal system. We measured contact angles of ionic liquid droplets with radii between some tens and some hundreds of nanometers by atomic force microscopy on an ideally flat silicon wafer. We found that the contact angles decreased with decreasing droplet size: smaller droplets showed stronger wetting. This dependence of the contact angle on the droplet radius could not be described with the concept of line tension or the modified Young's equation. We propose simple arguments for a possible alternative concept.

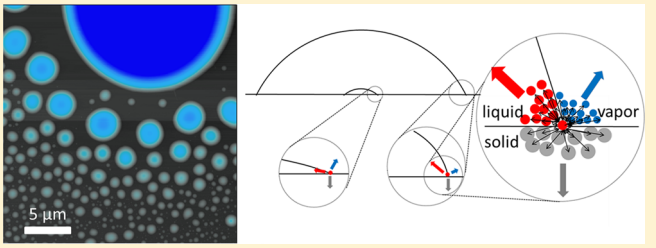

INTRODUCTION

In surface science, effects of interfacial tensions are of interest in numerous problems at different length scales, in both fundamental and applied science. Due to the downsizing of devices in engineering and fundamental research, there is a challenge to generate a deeper understanding of microscopic effects, in particular effects related to molecular origins—which cannot be seen at macroscopic scales. One example is how the contact angle of a sessile droplet depends on its size at nanoscopic or molecular dimensions. Whereas Young's equation,[1] though being challenged several times, is nowadays well-established and describes the relationship between the cosine of the contact angle and the interfacial tensions (liquid−vapor, liquid−solid, solid−vapor) on the macroscopic scale, this dependency is still under discussion for microscopic and smaller droplets. Due to different spatial arrangements of the molecules in the three-phase contact line (TPCL) and outside of it,[2] the molecular interactions—and with this their energy—differ. To take this into account, Young's equation has been modified by introducing a new parameter, the "line tension", which acts as an equivalent of the surface tension (plane) on the TPCL (line). Looking at the magnitude of the involved forces—which are mainly of van der Waals, electrostatic, and steric origins—it is obvious that line tension is only relevant on very small scales: either for droplets with radii in the submicrometer range, or for curvatures of the contact lines on that scale.[3,4] Those may be caused on purpose or by material-induced surface heterogeneities. The heterogeneities can be physical (roughness) or chemical (inhomogeneity of the surface material). Analyses on such small scales have been fragmentary for some time because of the lack of appropriate techniques. Experimental techniques with high sensitivity in the vertical direction like ellipsometry, X-ray reflectivity, or other scattering methods do not provide the lateral resolution needed to detect size effects on the contact angles of droplets. However, high-resolution scanning electron microscopy (SEM) as well as high-resolution atomic force microscopy (AFM) imaging now allows measurements with high lateral resolution at the nanoscale. AFM offers the advantage that surface topography is directly measured as 3D data by raster scanning the surface with a sharp tip, allowing for a quantitative analysis. Not only imaging, but also the manipulation of droplets at the nanometer scale on surfaces, for example, with scanning polarization force microscopy (SPFM) has been achieved by the use of this technique.[5]

We used AFM to investigate the relation between the contact angle and the size of nanodrops of an ionic liquid. Ionic liquids are salts in liquid state at room temperature with very low vapor pressure and high surface tension. These properties arise due to ionic bonding in the liquid that is stronger than van der Waals forces which act between molecules of other simple liquids. These properties also ensure that droplets do not evaporate during experiments, and form nonzero contact angles on a silicon surface.

Received: August 1, 2013
Revised: October 14, 2013

dx.doi.org/10.1021/la402932y | Langmuir XXXX, XXX, XXX−XXX

The size dependence of the wetting behavior for microscopic droplets is described by the "modified Young's equation":[6,7]

$$\cos\theta = \frac{\gamma_{SV} - \gamma_{SL}}{\gamma_{LV}} - \frac{\tau}{\gamma_{LV} r} = \cos\theta_{\infty} - \frac{\tau}{\gamma_{LV} r} \quad (1)$$

Here, θ is the equilibrium contact angle of the microscopic droplet, γ_{mn} stands for the surface energies of the three different interfaces: SV solid−vapor, SL solid−liquid, and LV liquid−vapor, respectively. r is the radius of the TPCL, θ_{∞} is the equilibrium contact angle of a macroscopic drop (Figure 1), and τ is the line tension.

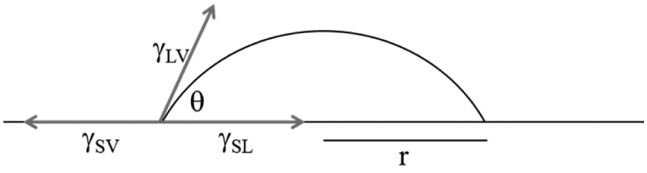

Figure 1. Schematic illustration of the cross section of a droplet on a surface.

The concept of line tension was introduced in the seventies of the 19th century by Josiah Willard Gibbs[8] to take the contribution of the TPCL into account while estimating the free energy for a droplet in equilibrium on a surface. Conceptually, the line tension (energy per line, J/m) is the two-dimensional equivalent of the surface tension (energy per area, J/m^2) for interfaces. A rough estimate for simple liquids (interacting only via intermolecular potentials) yields line tensions of the order of 10^{-11} J/m (3). However, in the literature, the algebraic sign of the line tension, and its order of magnitude vary widely in theoretical derivations and experimental investigations. Experimental values measured with different techniques cover a range of 7 orders of magnitude, from 10^{-12} to 10^{-5} J/m (2). If the line tension would be as small as 10^{-12} J/m, it would only have influence on systems with molecular dimensions. Larger values could influence processes on the micrometer scale, like heterogeneous nucleation, particle flotation, and cell adhesion.[9] It has been also shown that the magnitude of the experimentally determined line tensions changes with the size of the analyzed droplets, that is, large line tensions for larger droplets and smaller line tensions for smaller droplets.[10] Reasons for the broad range of the experimental values are most probably the variety of experimental approaches. Other possible reasons include differences in parameter characterization, and artifacts due to substrate heterogeneities that influence the measurements result in different values.[3] Most theoretical studies agree on a value of the order of 10^{-11} J/m. An upper limit of 5×10^{-9} J/m was calculated by Marmur based on energetic considerations and taking the change of the line tension with the contact angle into account.[11]

Special diligence has to be dedicated to the generation of the droplets. One requirement is that all analyzed droplets are generated in the very same way and show the same processing reaching their equilibrium state on the surface, that is, deposition is size-independent. On real surfaces the ideal (Young) contact angle, where the absolute minimum of the Gibbs free energy is reached, is flanked by values of local metastable minima, separated by energy barriers. This leads to a multiplicity of possible contact angles a droplet could potentially take on a surface. The extremes of the possible values for the contact angles are the receding (smallest) and the advancing (largest) contact angle. One can also distinguish between "theoretical" and "practical" values. "Theoretical" describes the values of the contact angles coinciding with the outermost minima of the Gibbs energy curve, which cannot be established in practice. Only the 'practical' values are achievable in experiments because there are always small energetic fluctuations in real systems.[12] Since also the deposition procedure determines the metastable energy minimum of the droplet, it is clear that the comparability of the deposition process of each individual droplet is of great importance for the outcome of contact angle measurements as a function of droplet size.

What approaches are promising? Microdroplets generated by spraying diluted liquids are unlikely to reach their equilibrium contact angles via identical processes. The evaporation of the solvent is influenced by the size of the droplets, leading to droplets with different concentrations of liquid and solvent on the surface. With different concentrations also different pinning effects of the contact line can occur (pinning occurs in the local minima of the Gibbs energy). Dilution is needed to allow the droplets to shrink to the desired nanosize by evaporation of the solvent, but this questions the comparability of droplets of different sizes. Undiluted ionic liquids, on the other hand, cannot be atomized to nanosizes because the required shearing force for droplet breakup cannot be applied via gas flow rate to the current nozzle dimensions. Droplets generated by film rupture[13,14] are affected by the problem that the moving contact lines of the droplets forming out of the ruptured film have to overcome pinning to reach equilibrium. Any mechanical deposition process where a volume of liquid is brought into contact with a surface, like by the use of nanopipets or AFM tips,[15,16] implies the breaking of a meniscus additionally to pinning effects. This makes it even more unlikely for the droplets to reach their equilibrium state in a size-independent manner, irrespective of the limitation concerning minimum droplet sizes that can be generated with this approach. To overcome this difficulty, we used a method of vaporization of pure ionic liquid to obtain equal conditions for the deposition of individual droplets in the size distribution investigated. By this approach we were able to generate and investigate droplets in equilibrium on solid substrates with diameters down to some tens of nanometers.

MATERIALS AND METHODS

Surface. A silicon wafer (100) p-type (CrysTec GmbH, Berlin, Germany) was used to provide an atomically flat reference surface for the investigations. The surface roughness of the silicon wafer was R_a = 2.6 nm, R_q = 3.2 nm measured on an area of 10 μm × 10 μm.

Liquid. 1-Butyl-3-methylimidazolium iodide [$C_8H_{15}IN_2$] (IOLITEC, Ionic Liquids Technologies GmbH, Heilbronn, Germany). This ionic liquid has a surface tension of 54.7 mN/m at 25 °C and a vapor pressure below -10^{-3} Pa at 20 °C. Investigating droplets with radii in the nanometer scale made it necessary to choose a liquid with such a low vapor pressure.

Droplet Generation and Deposition. A small drop of ionic liquid (spread to an area of approximately 0.8 cm^2) was placed on a piece of silicon wafer with an area of approximately 4 cm^2. This sample was put on a heating stage at a temperature of 250 °C. The boiling point of 1-butyl-3-methylimidazolium iodide is between 315 and 330 °C (datasheet). This heating produces a mist that is visible by the naked eye with appropriate illumination. With a clean silicon wafer surface a sample of droplets was picked up approximately 1 cm above the heated drop of ionic liquid. The face to be covered by nanodrops was directed versus the heated drop. This happened in less than a

dx.doi.org/10.1021/la402932y | Langmuir XXXX, XXX, XXX−XXX

second. We suppose that the droplets do not condense on the wafer surface but contact the wafer surface fully formed, so that the process of impacting the wafer surface is size independent. This procedure leads to a distribution of droplets in the size range between 20 nm and several hundreds of nanometers (Figures 2 and 3).

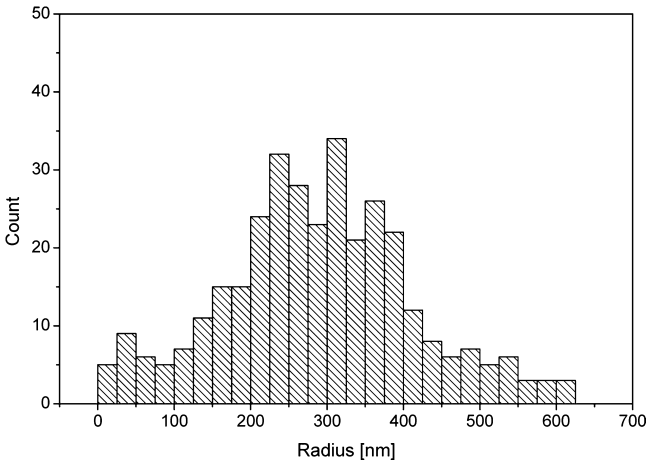

Figure 2. Size distribution of droplets of 1-butyl-3-methylimidazolium iodide on the silicon wafer surface.

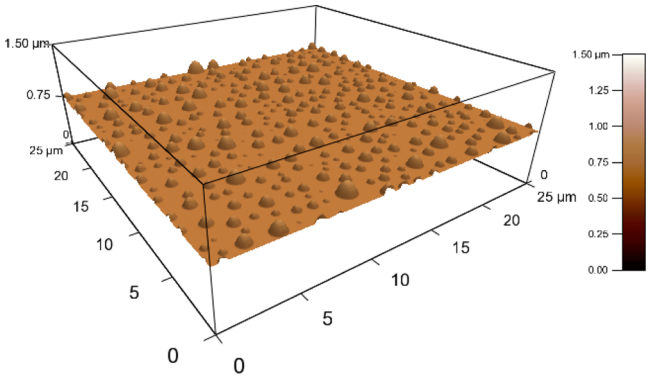

Figure 3. 3D AFM topography image of ionic liquid droplets on a silicon wafer. The scale in Z and XY is not the same.

All sessile droplets are far below the capillary length, have a spherical cap, show axial symmetry, and do not change their shape and size for months.

The contact angle can be determined from height h and radius r with the relation:

$$\theta = 2 \arctan\frac{h}{r} \qquad (2)$$

Droplet Imaging. We used an MFP-3D (Asylum Research, Santa Barbara, CA, USA) AFM for droplet topography imaging. The cantilever used was a SSS NCL (Super Sharp Silicon, NANOSENSORS, Switzerland) with a tip radius of typically 2 nm (manufacturer information). Imaging was done under usual laboratory ambient atmosphere in noncontact mode. The influence of the parameter settings for imaging will be discussed in more detail below.

Image Processing. The image to process is three-dimensional. For every horizontal point (x,y) the height (z) is given. The task for the analysis is to identify and evaluate every individual droplet. For this the deviation of the given vectors into "wafer surface vector" and "droplet vector" is required. To identify the "wafer surface vectors" in a first step the deviation of the used silicon surface from an ideal plane is accounted for by a special plane fitting procedure.

From the central region for both scanning directions (fast scan direction and slow scan direction) topography cross sections have been extracted. After eliminating the data points belonging to droplet contours from the data sets the remaining profiles have been fitted with polynomials of a higher order. Those contours have been used to generate polynomial surfaces in x and y directions, which were subtracted from the original height image data.

To identify the "droplet vectors" a height threshold (details see below) was determined. This height threshold transforms the height image (scale of 256 values) into a black and white image (2 values). By this the separation between wafer surface and droplets was attained. With this information the height image was analyzed to obtain the values of maximum height of the droplets, height of the perimeter of the base of the droplets on the wafer surface, and equivalent disc radii of the individual droplets. With the corrected droplet height values (maximum minus height of the perimeter of the base) we calculated the contact angles of the droplets in dependence of the radii with eq 2.

RESULTS AND DISCUSSION

Parameters Influencing Data Acquisition. It is known that the imaging parameters in noncontact AFM imaging of nanobubbles had a strong influence on the detected contours of the scanned liquid–vapor contact lines.[17] Thus we checked the influence of different parameter settings for our experiments with nanodrops. The drive amplitude determines the free oscillation of the cantilever; the set point gives the required damping due to the proximity of the surface. This damping is kept constant while scanning the surface, thus generating the desired height information of the topography. A first image was taken with relatively small drive amplitude and a set point that required only minor damping. Then we raised the drive amplitude in two steps by 25% and 50%. We did the same with the set point, adjusting the drive amplitude to ensure stable imaging. Image processing and data evaluation to determine the values of the line tension was performed as described before. The maximal deviation from the mean value of the line tension of these five measurements was 27%, with no evident dependence on the parameter settings. Thus the error of the determined line tension value is in the range of 25%. Keeping in mind that the debate is about algebraic signs and orders of magnitude, an error of this size due to varying the imaging parameters is certainly acceptable.

Parameters Influencing Data Analysis. To estimate to what extent the height threshold influences the evaluated values of line tension, we varied the height threshold by ±10%. Analyzing those data sets results in a change of the values for the line tension of 13% for the reduced threshold and 21% for the increased threshold. So changing this parameter for image analyzing on purpose by 10% results in a change of the determined line tension value of at most 21%. So also here the algebraic sign as well as order of magnitude are not affected by arbitrary variations of parameters in data processing.

In Figure 4 two regions can be distinguished. In the first region, where droplet radii are larger than ∼400 nm, the contact angle is nearly constant, independent of drop size. In the second region, for droplet radii smaller than ∼400 nm, contact angle decreases with drop size. All droplet sizes are several orders of magnitude below the capillary length $\lambda_c = (\gamma_{il}/\rho g)^{1/2}$ = 1.93 mm, with γ_{il} the surface tension (54.7 mN/m) and ρ the density (1.490 kg/m^3) of the ionic liquid 1-butyl-3-methylimidazolium iodide. It was shown that influences on the spherical shape of a sessile droplet could be noticeable for droplets larger than ∼10% of their capillary length.[18] In our study we are well below this value.

For comparison with the values of macroscopic droplets, we measured the advancing and receding contact angles by the

dx.doi.org/10.1021/la402932y | Langmuir XXXX, XXX, XXX–XXX

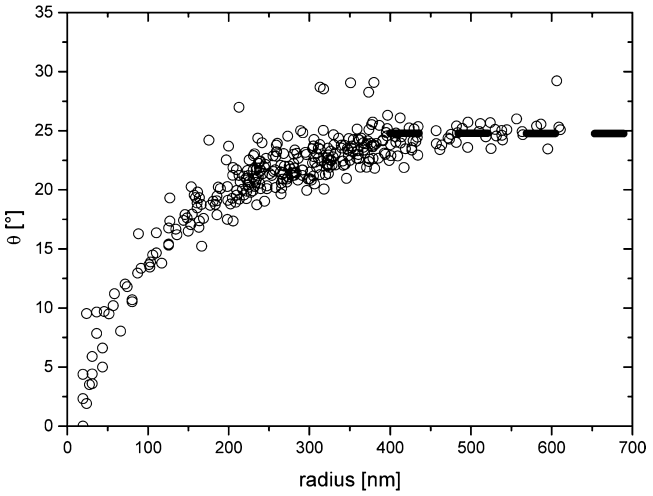

Figure 4. Contact angles versus radius for droplets of ionic liquid on a silicon wafer. The dashed line marks the range where a constant contact angle is reached.

sessile drop method (Drop Shape Analysis System DSA100, KRÜSS GmbH, Hamburg, Germany). Droplets radii were between 1 and 1.5 mm. Videos of the expansion and contraction of droplets of 1-butyl-3-methylimidazolium iodide on a silicon wafer have been recorded at three different positions. We obtained a value of 40 ± 4° for the advancing and 24 ± 2° for the receding contact angle (Figure 5). The value of

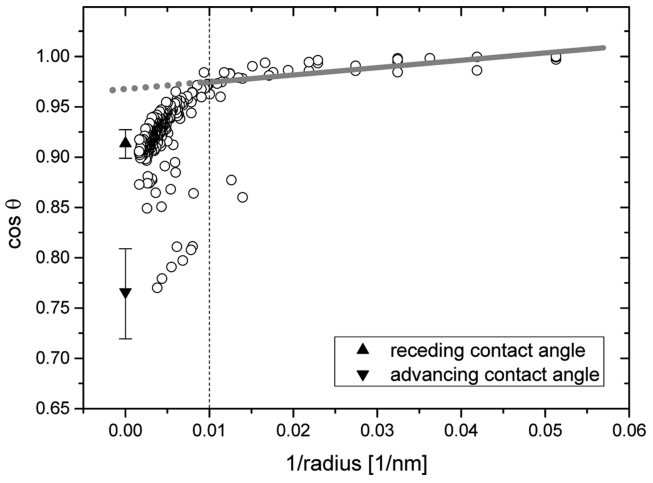

Figure 5. Cosine of the contact angle vs inverse of base radius of the droplets. Triangular symbols represent measured contact angles for macroscopic drops.

receding contact angle we determined for the macroscopic droplets corresponds, within errors, to the value of contact angles measured on the nanodroplets. In effect the angles measured on the nanodroplets are receding contact angles, as can be understood by looking at the impact dynamics of the droplets on the surface. Upon impacting on the surface, the droplet starts wetting the surface mainly driven by inertial (i.e., kinetic) forces.[19] After reaching the maximum spreading radius, the droplet starts recoiling due to surface tension. The system is overdamped, so that the drop base radius makes only one oscillation before reaching the local equilibrium in the receding contact angle state. Since this wetting process is independent of drop size, all droplets on the surface are "trapped" in the receding contact angle state.

One thing that differs between our results and other measurements of the contact angles as a function of droplet size to evaluate the line tension is the following: In most of the experimental data the cosine of the contact angle versus the inverse of the contact line radius shows a linear dependence, as predicted by the modified Young equation (eq 1). This is the case for experiments with droplets in different size ranges in the interval from 60 nm to about 550 μm.[9,20−25] Linearity is also hypothesized by fitting data of droplets with radii from 10 to 100 nm, even though the statistical spread of the values makes the conclusion not so unambiguous.[26] As the interval of investigated radii increases, the shortcoming of the linear fitting becomes apparent. Checco et al.[27] mentioned that a linear fit did not satisfactorily describe their data. There, a size range of a factor ∼20 was evaluated. In another measurement they investigated an interval of droplets in the size range from approximately 150 nm to 5 μm,[28] a factor of ∼30 in size. Also there nonlinearity was found, like in our case. The relative size ranges are comparable in their and our measurements, although the droplets presented here are on a smaller size scale—leading to a more pronounced nonlinearity in our case.

The determination of the line tension τ from the data was done by determining the slope of the data shown in Figure 5 plotted as $\cos(\theta)$ versus $1/r$, with r the radius of the contact line of the nanodrops. If the dependency is linear, as supposed by the modified Young's equation, a linear fit of all data is expected to give the most likely value. In our case, where the dependency showed up to be nonlinear (see Figure 5), we only used a section of the data points. Because the influence of the line tension is more pronounced for smaller droplets, we used only droplets with radii smaller than 100 nm for the fitting procedure. In this size interval a linear fit seems most reasonable (see Figure 5 and Supporting Information). This resulted in a value for the line tension of $\tau = -3.15 \times 10^{-11}$ J/m. The algebraic sign is negative, meaning that smaller droplets wet the surface stronger.

In the literature there are arguments for both algebraic signs for the line tension. Theoretical predictions give different signs depending on the model used. However, experimental investigations have also found both signs.[10] The determined value in our investigation is in agreement with theoretical approximations mentioned in the Introduction, claiming values in the order of 10^{-11} J/m.[3]

In the literature[26] the line tension τ is used as a fitting parameter to be considered as only the first order correction of Young's equation:

$$\cos\theta = \cos\theta_{\infty} - \frac{1}{\gamma_{LV}}[\tau\kappa + \chi\kappa^2 + ...] \quad (3)$$

where $\kappa = 1/r$.

Fitting our data with the first two terms in the bracket of eq 3 was not successful. Indeed, even the use of a third term did not allow us to match the dependency we found. Furthermore, the physical meaning of the higher order coefficients is not clear as well. However, further correction terms to the modified Young's equation as well as further experimental work have already been requested to answer further open questions concerning the behavior of droplets on the nanometer scale.[29]

So, to our knowledge, currently there is no model that can describe our experimental findings. The derivation of a

dx.doi.org/10.1021/la402932y | Langmuir XXXX, XXX, XXX−XXX

complete theoretical model is out of the scope of this paper; here, our main result is the demonstration that the modified Young equation is not sufficient for understanding our data. However, the arguments below illustrate that the change of the line tension with changing contact angle is not surprising.

Figure 6 illustrates the essentials for understanding the influence of the changing contact angle on line tension due to

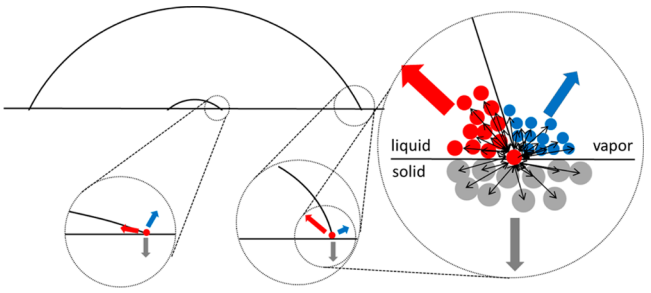

Figure 6. Sketch of different strength of forces on a molecule in the TPCL for different contact angles/droplet sizes. The differently colored arrows represent different intermolecular interactions between a molecule in the TPCL and its neighboring molecules.

the altered intermolecular forces. The molecules in the TPCL interact with their neighboring molecules. There are three different types of interactions relating to the three phases: solid, liquid, and gas. Clearly, with the changing contact angle, the magnitude of the interactions between the TPCL-molecules and liquid/gas phases also change significantly. Thus, the assumption that the value for line tension is a constant seems rather unjustified.

Also in the literature the assumption of a constant line tension is judged to be inappropriate, based on the simple theoretical argument that the intermolecular forces cannot be independent from the contact angle.[11]

Here, we provide a qualitative argument, emphasizing that the line tension must change in a more complex manner than postulated by the modified Young's equation. The magnitude of the line tension can be influenced by changing contact angles with droplet size when looking at the TPCL on the molecular level. Figure 6 illustrates the intermolecular interactions between a molecule in the TPCL and its neighbors, which are different for the three different phases. Concerning the line tension we only care about the competing components directing upward in this sketch, because they generate components parallel to the surface.

How could we make this illustration more quantitative? The vectors of interest are the bisecting lines of the angles of the segments (Figure 7). The resulting force of the projections onto the plane of contact has the proportionality given in eq 4.

$$F \sim A_a \cos(\alpha/2) - A_b \cos(\beta/2) \quad (4)$$

Figure 7 elucidates that the areas of interaction are proportional to the angles: $A_a \sim \alpha$, $A_b \sim \beta$; while $\alpha+\beta = 180°$. Inserting them in eq 4 we obtain the following proportionality:

$$F \sim \alpha \cos(\alpha/2) - p(180° - \alpha) \cos[(180° - \alpha)/2] \quad (5)$$

where the factor p takes account of the fact that the intermolecular forces acting on the molecules in the TPCL differ for the cases of identical or different neighboring molecules.

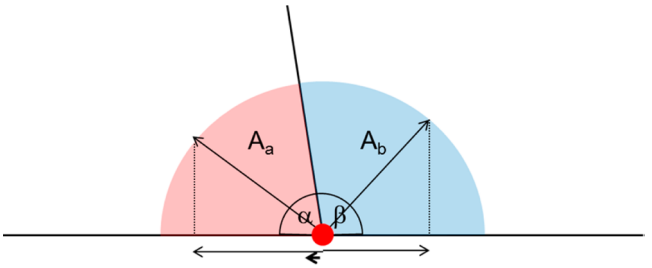

Figure 7. Sketch of the parameter relations used in eqs 4 and 5. A_a and A_b are areas of interaction of the molecule in the TPCL with its neighbors; α and β are angles between the surfaces. In the case of a droplet on the surface α corresponds to θ, A_a to the liquid, and A_b to the gas phase. The thin horizontal arrows are the projections of the bisecting lines, the components of the forces acting in the direction of the droplet center. The short thick arrow shows the resulting force.

This rough estimation of the relation between the involved forces and the contact angle illustrates that the magnitude as well as the algebraic sign of the first derivative of the resulting force acting radially on the molecules in the TPCL change with the contact angle. This behavior is influenced by the factor p. This is pictured in Figure 8, showing the results of eq 5 for

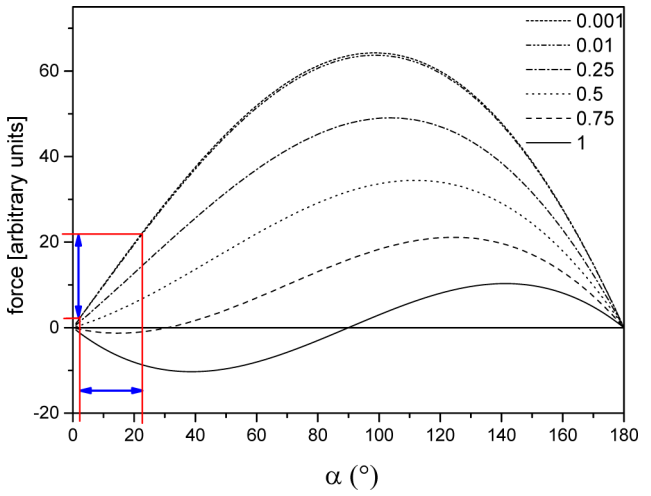

Figure 8. Resulting force acting on the molecule in the TPCL in relation with the contact angle and depending on the parameter p representing the relation between the involved intermolecular forces.

different values of p. If the forces are of the same strength a rotationally symmetric relation is the result. This is evident from the symmetry of the alignment in Figure 7. With increasing strength of the intermolecular interactions of identical molecules (i.e., when p decreases) the force toward the center of the droplet becomes dominant. At some point a further increase of the forces between identical neighboring molecules relative to different neighboring molecules does not change the relation any more. The two upper curves in Figure 8 are almost identical although there is 1 order of magnitude difference in the value of factor p.

We tried to evaluate the relation for the materials used in this experimental work: ionic liquid, silicon wafer, and air. Depending on the different relative orientations among the molecules, intermolecular forces at distances of 1 nm between two ionic liquid molecules were up to 3 orders of magnitude larger in comparison to the forces between ionic liquid molecules and the air molecules surrounding the droplet

dx.doi.org/10.1021/la402932y | Langmuir XXXX, XXX, XXX−XXX

(N2, O2) (internal communication). These large differences and the fact that the mean free path length of gas molecules is in the range of 60−70 nm indicate that a curve in the proximity of the asymptotic curve of Figure 8 (p = 0.01) is suitable for a rough estimation for the system investigated. An evaluation of the change of the force acting radially to the TPCL in the interval of the experimentally determined contact angles resulted in a decrease of the force of approximately 1 order of magnitude. This can be roughly estimated in the graphic of Figure 8 by following the upper curve from approximately 25° to 2.5°. This tendency is in agreement with the better wetting behavior for the smaller droplets we observed in the experiment. The determined values of the inclination in Figure 5 for the 20% smallest (20 nm; 136 nm) and 20% largest (484 nm; 600 nm) droplets investigated differ by a factor of 13.78. So the orders of magnitude from our measurements and from the illustration seem to agree. The qualitative behavior suggested by this model also could explain most of the observations of the size dependence of nanobubble contact angles.[30,17,,,32]

SUMMARY

We investigated the size dependence of the contact angle of nanodroplets of ionic liquid wetting a silicon wafer surface with AFM. The droplets analyzed were in the size range between tens and hundreds of nanometers. They were deposited with a vaporizing method that ensures that the droplet-deposition process was size independent, which is a basic requirement when the relation between contact angle and droplet size is investigated. We showed that the contact angle is depended on droplet size and that smaller droplets showed enhanced wetting, that is, a smaller contact angle. The determined value for the line tension was negative and of the order of 10^{-11} J/m. This order of magnitude agrees with previous theoretical considerations. We demonstrated that the influence of the AFM imaging parameters as well as the image data processing was of minor influence on the determination of the value of the line tension. The dependency of the cosine of the contact angle on the inverse of the radius showed a nonlinear behavior, contrary to some earlier experimental works. This experimentally found dependence could neither be described with the concept of the modified Young equation, nor with additional correction factors of higher order. We presented arguments why the line tension is not expected to be constant as droplet contact angles change. In particular, we have outlined a simple description showing how size dependence of contact angle might be understood. The qualitative trends of this model show agreement with the experimental data.

ASSOCIATED CONTENT

Supporting Information

Examples of circular fits to individual droplet profiles as well as linear fittings for different droplet size intervals. This material is available free of charge via the Internet at http://pubs.acs.org.

AUTHOR INFORMATION

Corresponding Author

*E-mail: heim@csi.tu-darmstadt.de.

Notes

The authors declare no competing financial interest.

ACKNOWLEDGMENTS

The authors thank Marcus Lopes and Subramanyan Namboodiri Varanakkottu for support in macroscopic contact angle measurements and Fereshte Taherian Tabasi for estimating the intermolecular forces. E.B. and L.O.H. acknowledge the support by the German Science Foundation (DFG) within the Cluster of Excellence 259 “Smart Interfaces - Understanding and Designing Fluid Boundaries”.

REFERENCES

(1) Young, T. An essay on the cohesion of fluids. *Philos. Trans. R. Soc. London* **1805**, *95*, 65−87.
(2) Drelich, J. The significance and magnitude of the line tension in three-phase (solid-liquid-fluid) systems. *Colloids Surf., A: Physicochem. Eng. Aspects* **1996**, *116* (1−2), 43−54.
(3) Quere, D. Surface wetting - Model droplets. *Nat. Mater.* **2004**, *3* (2), 79−80.
(4) Bonaccurso, E.; Butt, H.-J. Microdrops on atomic force microscope cantilevers: evaporation of water and spring constant calibration. *J. Phys. Chem. B* **2005**, *109* (1), 253−63.
(5) Hu, J.; Carpick, R. W.; Salmeron, M.; Xiao, X. D. Imaging and manipulation of nanometer-size liquid droplets by scanning polarization force microscopy. *J. Vac. Sci. Technol., B* **1996**, *14* (2), 1341−3.
(6) Boruvka, L.; Neumann, A. W. Generalization of classical-theory of capillarity. *J. Chem. Phys.* **1977**, *66* (12), 5464−76.
(7) Toshev, B. V.; Platikanov, D.; Scheludko, A. Line tension in 3-phase equilibrium systems. *Langmuir* **1988**, *4* (3), 489−99.
(8) Gibbs, J. W. On the equilibrium of heterogeneous substances. *Trans. Conn. Acad., Philos. Trans. R. Soc.* **1878**, *3*, 181.
(9) Amirfazli, A.; Kwok, D. Y.; Gaydos, J.; Neumann, A. W. Line tension measurements through drop size dependence of contact angle. *J. Colloid Interface Sci.* **1998**, *205* (1), 1−11.
(10) David, R.; Neumann, A. W. Empirical equation to account for the length dependence of line tension. *Langmuir* **2007**, *23* (24), 11999−2002.
(11) Marmur, A. Line tension and the intrinsic contact angle in solid-liquid-fluid systems. *J. Colloid Interface Sci.* **1997**, *186* (2), 462−6.
(12) Marmur, A. Soft contact: measurement and interpretation of contact angles. *Soft Matter* **2006**, *2* (1), 12−7.
(13) Sharma, A.; Reiter, G. Instability of thin polymer films on coated substrates: Rupture, dewetting, and drop formation. *J. Colloid Interface Sci.* **1996**, *178* (2), 383−99.
(14) Luo, C. X.; Xing, R. B.; Zhang, Z. X.; Fu, J.; Han, Y. C. Ordered droplet formation by thin polymer film dewetting on a stripe-patterned substrate. *J. Colloid Interface Sci.* **2004**, *269* (1), 158−63.
(15) An, S.; Stambaugh, C.; Kim, G.; Lee, M.; Kim, Y.; Lee, K. Low-volume liquid delivery and nanolithography using a nanopipette combined with a quartz tuning fork-atomic force microscope. *Nanoscale* **2012**, *4* (20), 6493−500.
(16) Fabie, L.; Ondarcuhu, T. Writing with liquid using a nanodispenser: spreading dynamics at the sub-micron scale. *Soft Matter* **2012**, *8* (18), 4995−5001.
(17) Borkent, B. M.; de Beer, S.; Mugele, F.; Lohse, D. On the shape of surface nanobubbles. *Langmuir* **2010**, *26* (1), 260−8.
(18) McHale, G.; Rowan, S. M.; Newton, M. I.; Banerjee, M. K. Evaporation and the wetting of a low-energy solid surface. *J. Phys. Chem. B* **1998**, *102* (11), 1964−7.
(19) Chen, L. Q.; Heim, L.-O.; Golovko, D. S.; Bonaccurso, E. Snap-in dynamics of single particles to water drops. *Appl. Phys. Lett.* **2012**, *100*.
(20) Amirfazli, A.; Hanig, S.; Muller, A.; Neumann, A. W. Measurements of line tension for solid-liquid-vapor systems using drop size dependence of contact angles and its correlation with solid-liquid interfacial tension. *Langmuir* **2000**, *16* (4), 2024−31.
(21) Amirfazli, A.; Keshavarz, A.; Zhang, L.; Neumann, A. W. Determination of line tension for systems near wetting. *J. Colloid Interface Sci.* **2003**, *265* (1), 152−60.

549 (22) Duncan, D.; Li, D.; Gaydos, J.; Neumann, A. W. Correlation of
550 line tension and solid-liquid interfacial-tension from the measurement
551 of drop size dependence of contact angles. *J. Colloid Interface Sci.* **1995**,
552 *169* (2), 256−61.
553 (23) Fery, A.; Pompe, T.; Herminghaus, S. Nanometer resolution of
554 liquid surface topography by scanning force microscopy. *J. Adhes. Sci.*
555 *Technol.* **1999**, *13* (10), 1071−83.
556 (24) Seemann, R.; Jacobs, K.; Blossey, R. Polystyrene nanodroplets. *J.*
557 *Phys.: Condens. Matter* **2001**, *13* (21), 4915−23.
558 (25) Wang, J. Y.; Betelu, S.; Law, B. M. Line tension approaching a
559 first-order wetting transition: Experimental results from contact angle
560 measurements. *Phys. Rev. E* **2001**, *63* (3), 031601.
561 (26) Berg, J. K.; Weber, C. M.; Riegler, H. Impact of negative line
562 tension on the shape of nanometer-size sessile droplets. *Phys. Rev. Lett.*
563 **2010**, *105* (7), 076103.
564 (27) Checco, A.; Schollmeyer, H.; Daillant, J.; Guenoun, P.;
565 Boukherroub, R. Nanoscale wettability of self-assembled monolayers
566 investigated by noncontact atomic force microscopy. *Langmuir* **2006**,
567 *22* (1), 116−26.
568 (28) Checco, A.; Guenoun, P.; Daillant, J. Nonlinear dependence of
569 the contact angle of nanodroplets on contact line curvature. *Phys. Rev.*
570 *Lett.* **2003**, *91* (18), 186101.
571 (29) Schimmele, L.; Dietrich, S. Line tension and the shape of
572 nanodroplets. *Eur. Phys. J. E* **2009**, *30* (4), 427−30.
573 (30) Yang, J. W.; Duan, J. M.; Fornasiero, D.; Ralston, J. Very small
574 bubble formation at the solid-water interface. *J. Phys. Chem. B* **2003**,
575 *107* (25), 6139−47.
576 (31) Kameda, N.; Nakabayashi, S. Size-induced sign inversion of line
577 tension in nanobubbles at a solid/liquid interface. *Chem. Phys. Lett.*
578 **2008**, *461* (1−3), 122−6.
579 (32) Yang, X.; Loos, J. Toward high-performance polymer solar cells:
580 The importance of morphology control. *Macromolecules* **2007**, *40* (5),
581 1353−62.